Target Diagnostics for Intense Lithium Ion Hohlraum Experiments on PBFA II

R. J. Leeper, J. E. Bailey, A. L. Carlson, G. A. Chandler, M. S. Derzon, R. J. Dukart, D. E. Hebron, L. P. Mix, A. R. Moats, T. J. Nash, W. R. Olson, C. L. Ruiz, J. A. Torres, and D. F. Wenger, Sandia National Laboratories, Albuquerque, NM 87185

R. W. Olsen, EG&G Energy Measurements, Kirtland Operations, Albuquerque, NM 87196

T. L. Barber, P. W. Lake, and F. A. Schmidlapp, Ktech Corporation, Albuquerque, NM 87110

Abstract

A review of the diagnostics used at Sandia National Laboratories to measure the parameters of intense lithium ion-beam hohlraum target experiments on PBFA II will be presented. This diagnostic package contains an extensive suite of x-ray spectral and imaging diagnostics that enable measurements of target temperature and x-ray output. The x-ray diagnostics include time-integrated and time-resolved pinhole cameras, energy-resolved 1-D streaked imaging diagnostics, time-integrated and time-resolved grazing incidence spectrographs, a transmission grating spectrograph, an elliptical crystal spectrograph, a bolometer array, an eleven-element x-ray diode (XRD) array, and an eleven-element PIN diode detector array. The incident Li beam symmetry and an estimate of incident Li beam power density can be measured from ion beam-induced characteristic x-ray line emission and neutron emission.

I. Introduction

Experimental programs to develop high-power light ion beams for use as an inertial confinement fusion (ICF) driver are underway at Sandia National Laboratories' Particle Beam Fusion Accelerator II (PBFA II) as well as at a number of other laboratories worldwide.[1] Light-ion ICF offers an efficient and potentially low-cost alternative to the laser and heavy-ion approaches to inertial fusion. Recent experiments on PBFA II have focused Li^+ ion beams to power densities equivalent to 1.5 TW/cm^2 averaged over the surface of a 6-mm-diameter spherical target in a 12-15 ns (FWHM) pulse at a peak voltage of 10 MeV. We are presently employing these beams to perform ion-beam heated target experiments at this facility.

Fig. 1 schematically shows a typical target and Fig. 2 shows the experimental arrangement used in our lithium ion beam heated target experiments. The radial Li^+ ion beam is emitted from the cylindrical anode surface of radius 15.5 cm and made incident on the conic target from a full 360 degrees of azimuth with a vertical extent that is typically $\pm$ 17 degrees. The beam passes through the 1 μm parylene and 0.5-1 μm gold walls of the target and due to dE/dx energy losses, is finally stopped in the 3-6 mg/cm^3 CH foam region of the target. The rapid beam heating of the foam causes it to ionize and emit soft x-ray radiation. This soft x-ray emission in turn heats the gold walls of the target which reradiate creating an x-ray radiation cavity or hohlraum. To date, target temperatures of 58 eV have been measured in these experiments. This paper describes the comprehensive

DISCLAIMER

Portions of this document may be illegible in electronic image products. Images are produced from the best available original document.

diagnostic package shown in Fig. 2 that has been developed to measure the performance of these hohlraum targets.

II. Intense Ion Beam Diagnostics

A filtered PIN array, several time-integrated x-ray pinhole cameras, and a neutron time-of-flight (TOF) diagnostic have been developed to measure the incident Li beam on our targets. These diagnostics are schematically shown in Fig. 2. The neutron TOF diagnostic operates by measuring neutrons produced by the incident beam in a number of target materials.[2] The PIN array and x-ray pinhole camera diagnostics operate by observing the lithium ion-induced inner-shell x-ray fluorescence from a titanium-coated strip located just outside the target (designed to yield the vertical profile of the beam) and on the gold cone of the inner target. This data is then used to extract the incoming beam's time history, vertical focus position, beam width, and azimuthal symmetry from shot to shot. Further details of these diagnostics are described in a companion article.[3] Direct lithium beam intensity measurements using an ion movie camera and a magnetic spectrograph to detect Rutherford-scattered ions have also been attempted. Interpretation of the data from these diagnostics was complicated by the steep cone angle of the conical target. Analysis of this data is continuing. The use of these diagnostics on flat gold targets is described in Ref. 2.

III. Total X-ray Fluence Diagnostic

A three element x-ray bolometer array diagnostic has been developed to measure the x-ray radiation fluence emitted by our targets. This diagnostic was derived from the bolometer concept of Degnan[4] and a description of our design is given by Hanson in Ref. 5. Each bolometer in the array consists of a thin 1 μm Ni film whose resistance increases as an approximately linear function of absorbed x-ray energy. To operate the bolometer, a bias current of 40 A is pulsed in the thin Ni film and the radiation x-ray source is discharged at the peak of this bias current. The incident x-ray radiation heats the film and the resulting resistive voltage change across the bolometer foil provides a measure of the absorbed x-ray radiation energy fluence.

IV. X-ray Imaging Diagnostics

A. Time-Resolved and Time-Integrated X-ray Pinhole Camera Diagnostics

The schematic of the time-resolved x-ray pinhole camera (TRXPC) is shown in Fig. 3a. This camera was developed to obtain time-resolved images of soft x-ray emission from an ion-beam-driven target in the spectral range of 100 eV to 900 eV. The camera operates by forming 36 pinhole images of the target soft x-ray emission target in groups of four onto nine separate micro-channel plate striplines in the image plane. The four image groups formed on each MCP stripline are spectrally resolved by broadband x-ray filters located in front of the camera's pinhole aperture plate (Fig. 3a). Typical x-ray spectral cuts are at 200 eV, 270 eV, 450 eV, and >800 eV. The MCP is DC biased at 150 V and each stripline is gated sequentially on with a nominal 350 V pulse. The interframe time of 5 ns is set by cable delay and the dwell time of each frame is 2 ns. The output of the MCP is the standard phosphor/fiber optic/film arrangement. Because of the blackbody character of the spectrum being observed, the response of the camera is balanced by using smaller 0.05 mm diameter pinholes in the low energy channel of the instrument, 0.13 mm diameter pinholes in the mid-energy channels, and 0.25 mm diameter pinholes in the high energy channel of the instrument. Consequently, the spatial resolution varies from low energy channels to high energy channels, but is typically 700-800 μm at the source which is adequate for our mm scale targets. Data from PBFA II shot 5942 is shown in Fig. 3b showing enhanced x-ray emission from the gold walls of the target. A number of time-integrated soft x-ray pinhole cameras are also fielded as part of PBFA II target experiments.

B. Streaked Fiber Array 1-D Imaging Diagnostic

A schematic of a typical arrangement of the time-resolved streaked fiber array 1-D imaging diagnostic is shown in Fig. 4.[6] This diagnostic was developed to obtain temporally continuous 1-D images of the ion beam target. The diagnostic operates by forming a 1-D slit image of the target onto three separate regions of a scintillator/fiber optic array image plane. The three images formed on the fiber optic array are spectrally resolved by broadband x-ray filters located just in front of the fiber optic bundle. Note that the slit integrates the emission from the target along the dimensions of the slit. The scintillator used is BC-418 plastic scintillator that is 20 μm thick. The coherent fiber array is 50 m long and consists of 30 fibers per spectral cut that are 100 μm in diameter. The fiber optic bundle is proximity coupled to the scintillator as shown. The output of the fiber bundle is lens coupled onto the photocathode of a streak camera. The output of the streak camera is lens coupled to a CCD camera.

V. X-ray Spectral Diagnostics

A. XRD Array Diagnostic

Broadband x-ray spectral measurements of soft x-ray emission from our targets are performed with an eleven element x-ray diode detector (XRD) array. These detectors have been designed and built at Sandia and are similar in design to those discussed in Refs. 7 and 8. This diagnostic measures target temperature from blackbody emission in the spectral range 30 eV to 1 keV. X-ray filters in front of the detectors provide broad energy cuts ($\Delta E/E$=0.5-1.0). The time resolution of these detectors is approximately 1 ns FWHM, ~20 times shorter than the measured radiation pulse. The spectral cuts are unfolded to produce a soft x-ray spectrum. A brightness temperature estimate is made from the total flux measured in the spectrum and the measured emission source size.

B. Transmission Grating Spectrograph

A schematic of the time-resolved transmission grating spectrograph is shown in Fig. 5. This spectrograph was developed at Sandia to obtain time-resolved spectra of continuum soft x-ray emission from our ion-beam driven targets in the spectral range of 50 eV to 1 keV with a source-size-limited resolution $\lambda/\Delta\lambda$ of 10 at 300 eV. The instrument operates by slit imaging the x-ray emission of the target onto an x-ray transmission grating. The transmission grating then energy disperses the incident x-rays by diffraction onto an MCP image plane that contains nine 50 ohm striplines. The x-rays are primarily dispersed into zeroth and first orders. The zeroth order diffraction pattern is simply a 1-D image of the target. The x-ray spectrum is obtained from x-rays dispersed into first order. The transmission grating used is a free-standing gold grating 0.3 μm thick with a 0.2-μm period.[9] Each MCP stripline has an effective dwell time of 1 ns and an interframe time set by cable delay of 6 ns.

C. Time-resolved and Time-Integrated Grazing Incidence Spectrographs

As shown in Fig. 2, time-integrated and time-resolved versions of grazing incidence spectrographs are used for high resolution measurements of the x-ray spectrum emitted in PBFA II target experiments in the spectral range 15 eV to 1 keV.[10] The higher resolutions of these spectrographs enable the utilization of standard line ratio and line broadening techniques to infer source temperature and density. The time-resolved spectrograph is a micro-channel plate intensified grazing incidence spectrograph (McPIGs) that is mounted on a 0.5 m radius Rowland circle.[11] An imaging slit forms a 1-D image of the target onto a spherical, 2 degree of angle-of-incidence gold coated mirror. The mirror in turn images these x-rays onto a slit that is immediately adjacent to the diffraction grating located on the Rowland circle. X-rays are dispersed by the diffraction grating onto a 15.2-cm. long, 0.5 m radius curved micro-channel plate that is on the Rowland circle. The MCP has six 25 ohm striplines coated onto its front surface that provide six spectral time gates. These striplines are operated at dwell times of 3 ns and an interframe time of 8 ns. The energy resolution of the spectrograph is $\lambda/\Delta\lambda$ of 100. The time-integrated spectrograph is identical to the McPIGs design with the exception of replacing the MCP detector with x-ray film.

D. Elliptical Crystal Spectrograph

An elliptical crystal spectrograph has been developed to measure the spectrum of x-rays emitted from our targets in the range of 700 eV to 10 keV. The primary goal of this instrument is to utilize either standard line-ratio techniques to infer the source temperature and density, or to use the beam induced characteristic line emission which can also be a sensitive indicator of source temperature. The spectrograph is a 0.49-m focal-length instrument using Johann focusing to minimize source-size effects.[12] The nominal spectral and spatial resolution of this instrument is $\lambda/\Delta\lambda$=1500–2000 and 1 mm, respectively.

VI. Summary

Intense lithium beam hohlraum target experiments are currently being conducted on the PBFA II facility at Sandia National Laboratories. A comprehensive diagnostic package has been developed that enables the measurement of the performance of these targets including incident beam, x-ray output, and target temperature.

VII. Acknowledgments

The authors would like to thank the PBFA-II operations crew for invaluable technical assistance and to thank Mona L. Aragon for her outstanding technical illustration work. This work supported by the U. S. Department of Energy under Contract No. DE-AC04-94AL85000.

References

1. D. L. Cook et al., Proceedings of Fourteenth International Conference On Plasma Physics and Controlled Nuclear Fusion Research, Wurzburg, Germany (1993) p. 63.
2. R. J. Leeper et al., Rev. Sci. Instrum. 59, 1860 (1988).
3. A. R. Moats et al., Rev. Sci. Instrum., these proceedings.
4. J. H. Degnan, Rev. Sci. Instrum. 50, 1223 (1979).
5. D. L. Hanson, "Users' Guide To The SNL Bolometer," Sandia National Laboratories (unpublished).
6. M. S. Derzon et al., 1993 SPIE International Symposium on Optical Instrumentation and Applied Science, SPIE Vol. 2002, 31 (1993).
7. R. B. Spielman and J. P. Anthes, AIP Conf. Proc. No. 75, 278 (1981). A Study of Bare Aluminum X-Ray Diode Saturation Due To A High Fluence X-Ray Pulse (4 Pages)
8. R. H. Day et al., J. Appl. Phys. 52, 6965 (1981).
9. X-OPT Inc., 2426 N.W. 26th Place, Gainesville, FL 32605.
10. B. McDonald, Spectral Precision, 1087 Fife Ave., Palo Alto, CA 94303.
11. D. L. Matthews et al., Phys. Rev. Lett. 54, 110 (1985)
12. B. A. Hammel et al., Rev. Sci. Instrum. 61, 1920 (1990).

Figure Captions

Fig. 1. Schematic of cone target used in intense lithium hohlraum target experiments on PBFA II.

Fig. 2. Schematic of experimental arrangement used in lithium hohlraum target experiments on PBFA II.

Fig. 3a. Schematic of soft x-ray framing camera.

Fig. 3b. Data obtained with soft x-ray framing camera on PBFA II Shot No. 5942 showing enhanced soft x-ray emission from the gold walls of the target.

Fig. 4. Schematic of streaked fiber array 1-D imaging diagnostic.

Fig. 5. Schematic of transmission grating spectrograph.

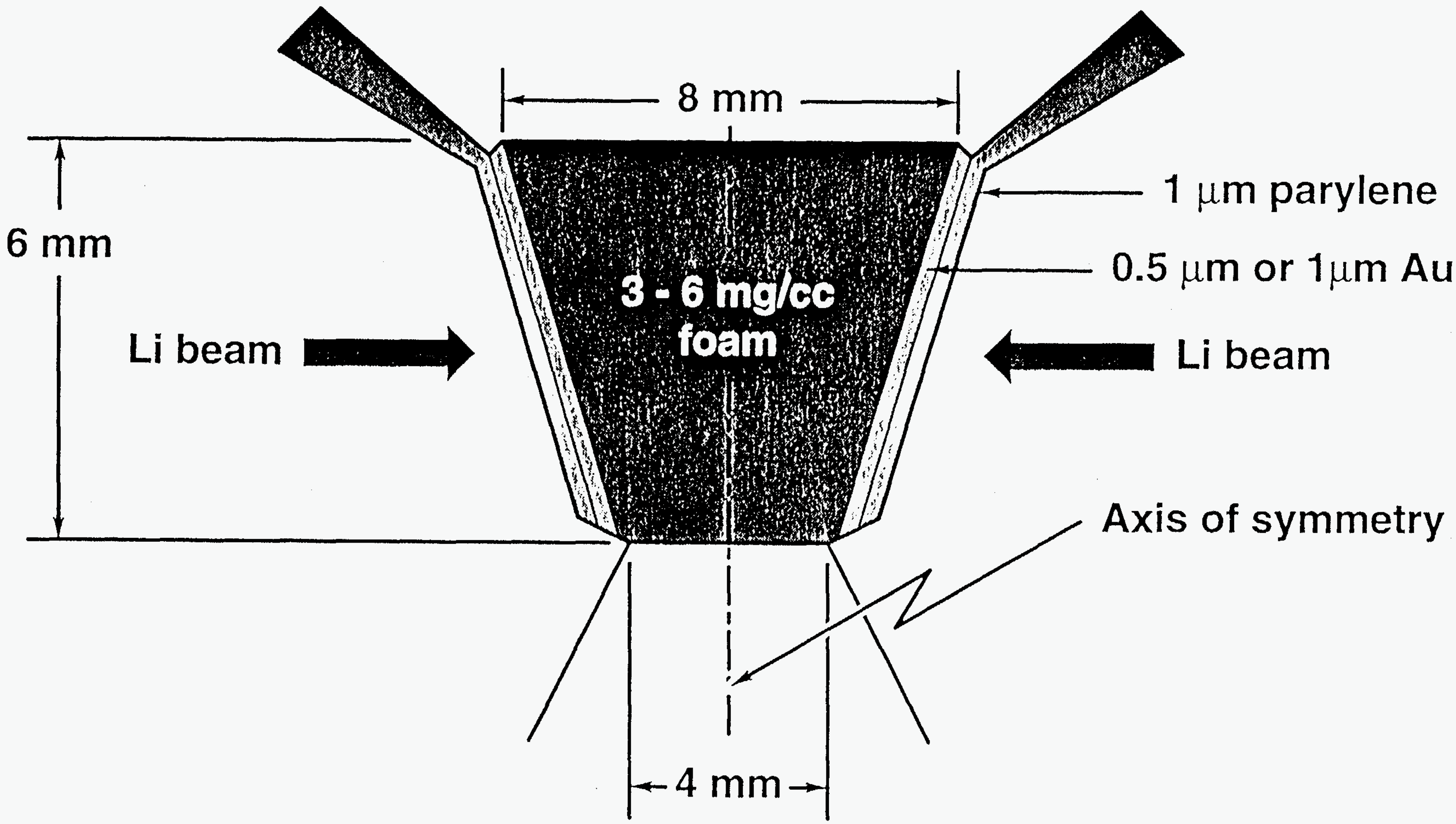

T.301.J.BW7609.02

Figure 1

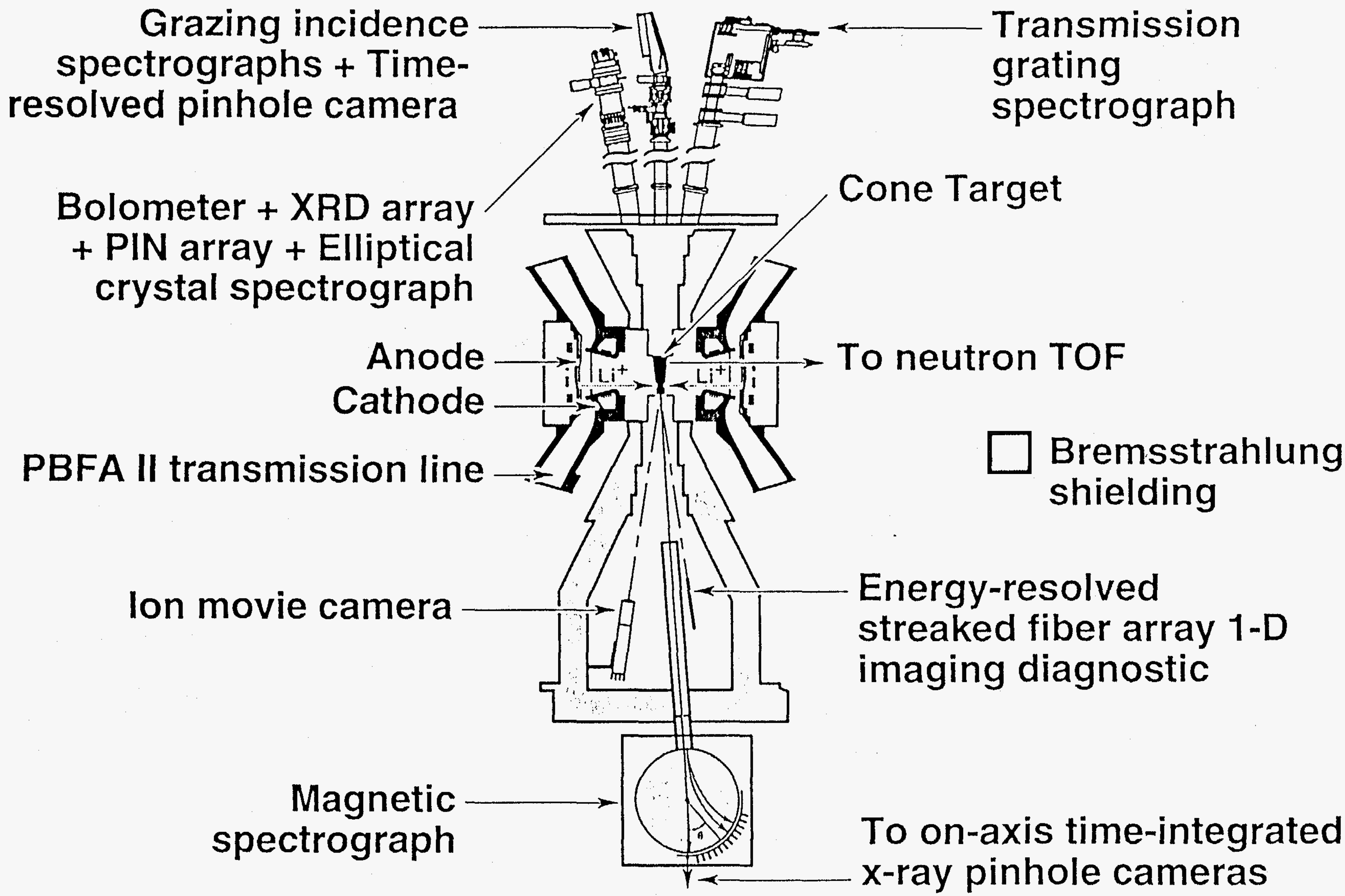

T.301.J.BW7609.03.

Figure 2

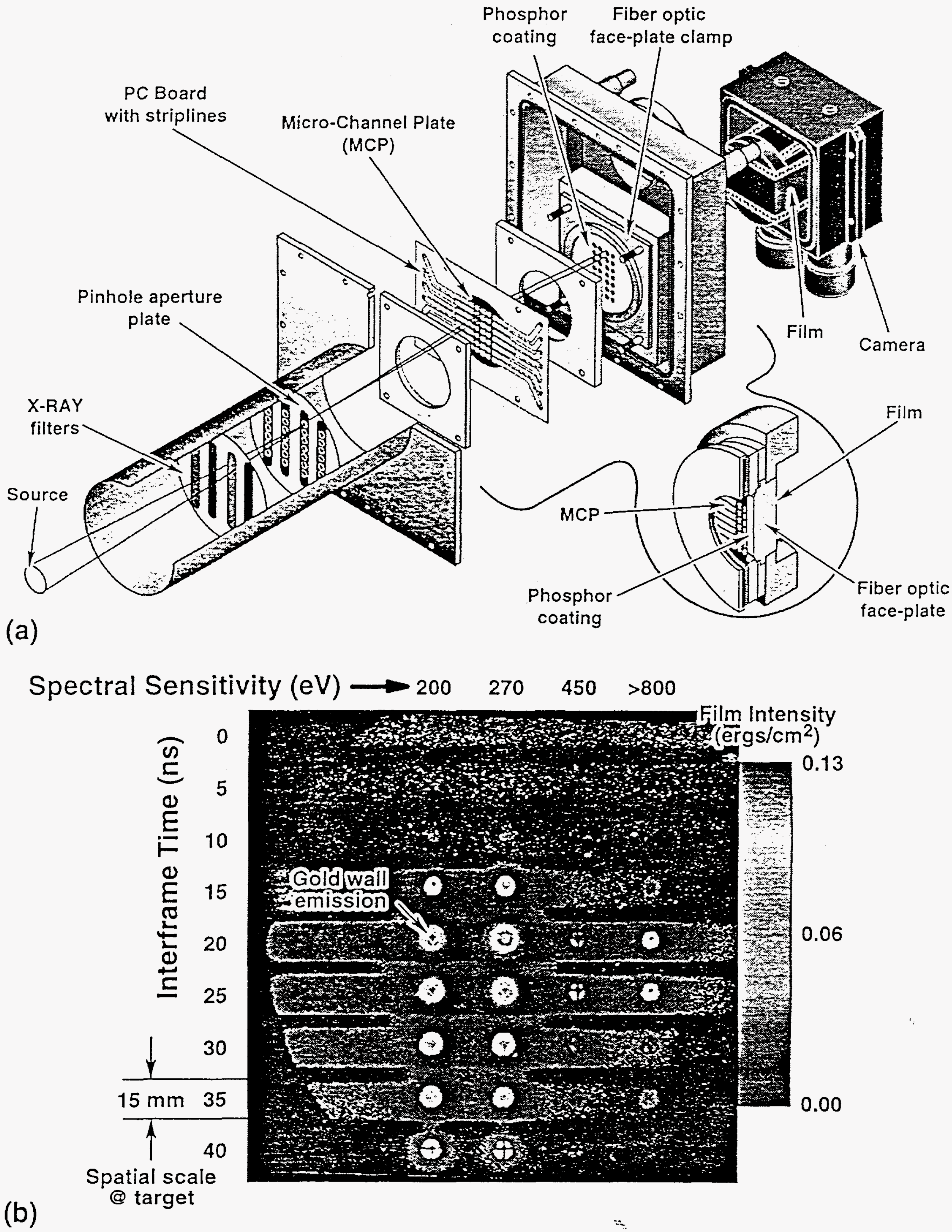

T.301.J.BW7609.13N

Fig 3

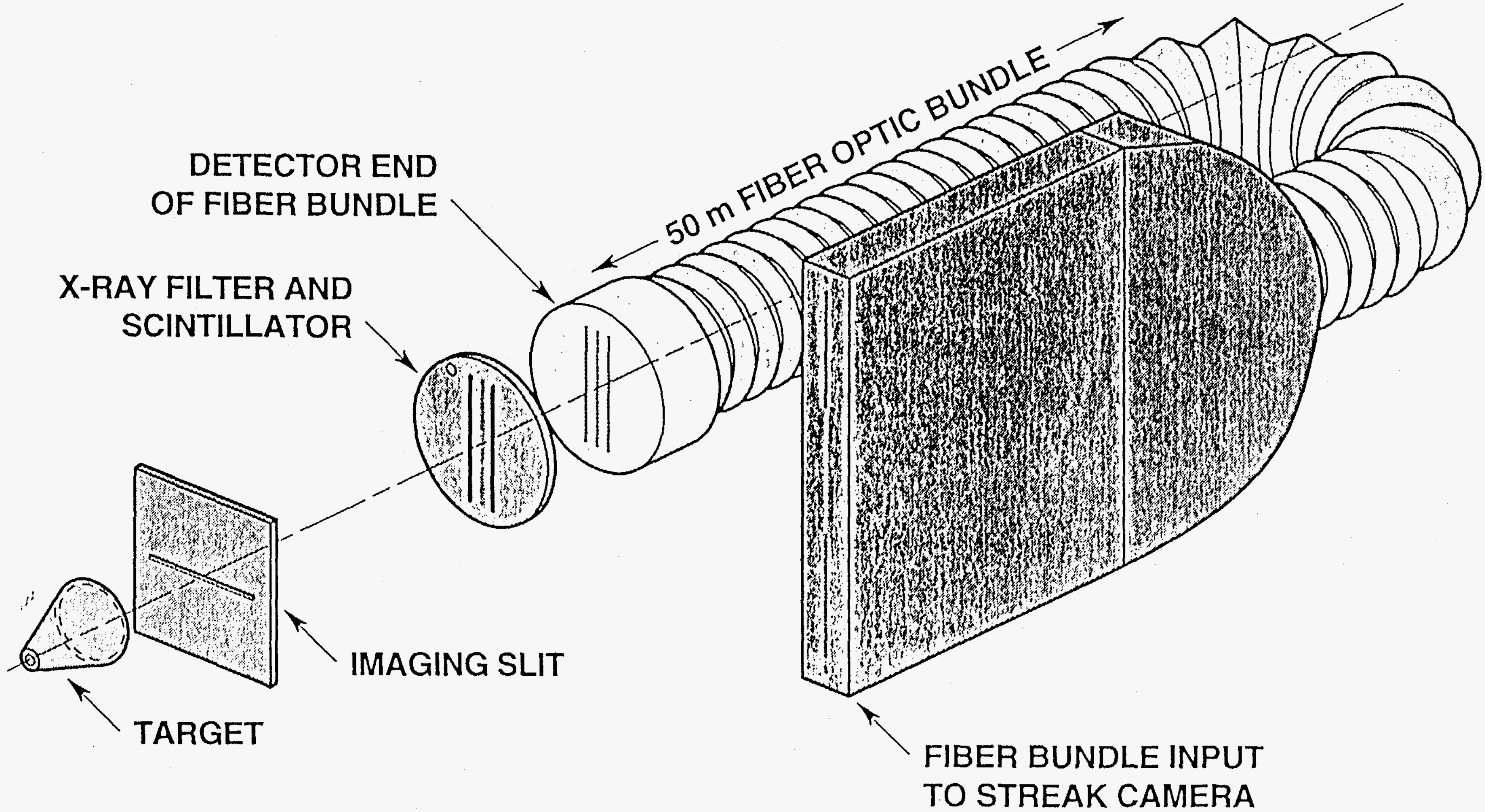

T.301.J.BW7609.12

Figure 4

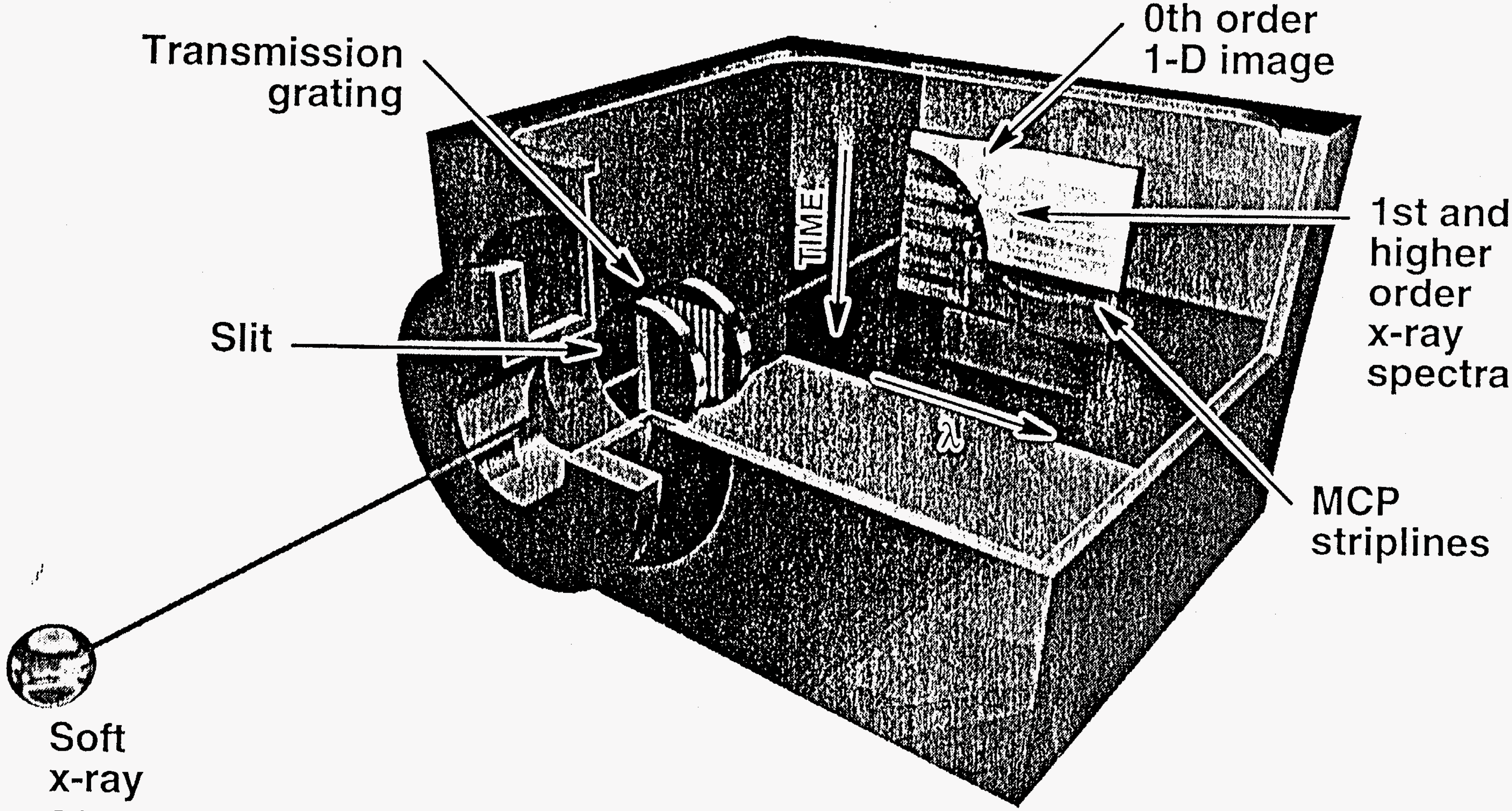

T.301.J.BW7609.22

Figure 5